Environ. Sci. Technol. **2005**, *39,* 6698−6704

Coupled Fe(II)−Fe(III) Electron and Atom Exchange as a Mechanism for Fe Isotope Fractionation during Dissimilatory Iron Oxide Reduction

HEIDI A. CROSBY,* CLARK M. JOHNSON, ERIC E. RODEN, AND BRIAN L. BEARD

Department of Geology and Geophysics, University of Wisconsin-Madison, 1215 West Dayton Street, Madison, Wisconsin 53706

Microbial dissimilatory iron reduction (DIR) is an important pathway for carbon oxidation in anoxic sediments, and iron isotopes may distinguish between iron produced by DIR and other sources of aqueous Fe(II). Previous studies have shown that aqueous Fe(II) produced during the earliest stages of DIR has δ^{56}Fe values that are 0.5−2.0‰ lower than the initial Fe(III) substrate. The new experiments reported here suggest that this fractionation is controlled by coupled electron and Fe atom exchange between Fe(II) and Fe(III) at iron oxide surfaces. In hematite and goethite reduction experiments with *Geobacter sulfurreducens*, the ^{56}Fe/^{54}Fe isotopic fractionation between aqueous Fe(II) and the outermost layers of Fe(III) on the oxide surface is ∼ −3‰ and can be explained by equilibrium Fe isotope partitioning between reactive Fe(II) and Fe(III) pools that coexist during DIR. The results indicate that sorption of Fe(II) to Fe(III) substrates cannot account for production of low-δ^{56}Fe values for aqueous Fe(II) during DIR.

Introduction

Microbial dissimilatory iron reduction (DIR) is a common biogeochemical process in modern and perhaps ancient anoxic environments (*1*−*3*) and results in the reductive dissolution of Fe(III) oxides/hydroxides such as ferrihydrite, goethite, and hematite. Experiments with dissimilatory iron-reducing bacteria have shown isotopic fractionations of approximately −1.3‰ in ^{56}Fe/^{54}Fe ratios between dissolved Fe(II) and the initial ferric oxide substrate (*4*, *5*), raising the possibility that Fe isotopes may be used to trace biological processing of Fe. Low-δ^{56}Fe values are commonly observed in dissolved and exchangeable Fe in soils (*6*−*8*), and pore fluids in modern marine sediments (*9*), and are inferred to have existed in ancient marine pore fluids from analysis of banded iron formations and black shales (*4*, *10*, *11*). Several pathways have been suggested for production of low-δ^{56}Fe values in aqueous Fe(II) in natural systems, including DIR (*4*, *5*, *10*−*13*), preferential sorption of isotopically heavy Fe(II) (*7*, *14*), and precipitation of high-δ^{56}Fe ferric oxides/hydroxides (*15*). A better understanding of the underlying mechanisms of Fe isotope fractionation during DIR and sorption will facilitate interpretation of Fe isotope measurements in natural settings.

DIR requires transfer of electrons to insoluble iron oxides, either through direct reduction at the microbial surface, chelation of Fe(III) followed by extracellular or periplasmic reduction, or indirect reduction via electron shuttles (*16*). *Geobacter* species require direct contact with the oxide surface, whereas *Shewanella* species and *Geothrix fermentans* can utilize low molecular weight electron-shuttling compounds and possibly Fe(III) chelators, potentially eliminating the need for cellular contact with the oxide surface (*17*−*20*). Yet, Fe isotope studies using *Geobacter* and *Shewanella* species with acetate and lactate as the electron donor, respectively, showed similar isotopic fractionations when a common electron acceptor (ferrihydrite) was used (*13*). Addition of the humic acid analogue 2,6-anthraquinone disulfonate (AQDS), a soluble electron shuttle that facilitates indirect Fe oxide reduction, appears to have no effect on Fe isotope fractionations during DIR (*14*). These observations suggest that fractionation between aqueous Fe(II) and oxide substrate may not be dependent on the biochemical method of Fe(III) reduction. This is dissimilar to other biological isotope fractionations, such as sulfur isotope fractionation by sulfate-reducing bacteria, which are heavily dependent on biochemical pathways and type of electron donor (*21*, *22*).

Based in part on the evidence that at least some species of bacteria solubilize Fe(III) during DIR (*17*, *18*), Beard et al. (*5*) hypothesized that the −1.3 ‰ fractionation in ^{56}Fe/^{54}Fe ratios measured between $Fe(II)_{aq}$ and initial ferric oxide/hydroxide substrate may primarily reflect isotopic fractionation between pools of ligand-bound Fe(III) and Fe(II) that are open to isotopic exchange (Figure 1). If dissolution of the ferric Fe substrate occurs congruently, there should be no isotopic fractionation during this step (*12*). However, because significant isotopic fractionation occurs between ferric and ferrous species (*23*−*25*), Fe isotope exchange between ligand-bound or aqueous Fe(II) and ligand-bound Fe(III) (Δ_1 in Figure 1A) was envisioned as the most likely mechanism by which isotopic fractionation may occur during DIR. Alternatively, it has been proposed that Fe isotope fractionation during DIR could be driven by Fe(II) adsorption to the Fe oxide surface (Δ_2 in Figure 1A), where the fractionation between adsorbed and aqueous Fe(II) was calculated (but not directly measured) to lie between +2‰ and +5‰ (*14*).

A third mechanism that has been suggested but not previously investigated is Fe isotope fractionation during interfacial electron transfer and atom exchange between adsorbed or aqueous Fe(II) and a reactive Fe(III) pool on oxide surfaces (Figure 1B) (*14*, *26*). Several studies speculated that interfacial electron transfer may occur between adsorbed Fe(II) and Fe(III) oxides/hydroxides (*27*−*32*), and recent work using Mössbauer spectroscopy provides direct evidence for interfacial electron transfer (*26*). An important distinction between the two models illustrated in Figure 1 is that Fe in the ferric substrate is not envisioned to have undergone isotopic exchange in the "ligand fractionation model" (Figure 1A), whereas if electron exchange with the ferric substrate occurs, as in the "substrate redox cycling model" of Figure 1B, participation of the ferric substrate in isotopic exchange should produce an isotopically zoned ferric substrate.

In this study, stable isotope methods were used to investigate the possibility that Fe isotope fractionation occurs during redox cycling at the oxide surface, which allows calculation of the size of the Fe pools that are open to atom exchange. *G. sulfurreducens* was chosen for these experiments because members of the *Geobacteraceae* family are the most common Fe reducing bacteria in natural environments in which community structure has been analyzed (*33*−*35*),

* Corresponding author phone: (608)262-8960; fax: (608)262-0693; e-mail: heidic@geology.wisc.edu.

10.1021/es0505346 CCC: $30.25
Published on Web 07/23/2005

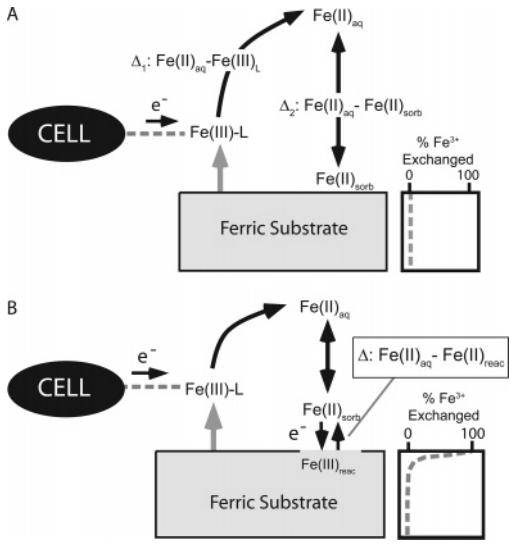

FIGURE 1. Conceptual models for Fe isotope fractionation during DIR and graphical representation of the extent of Fe(III) exchange between the oxide surface and sorbed Fe(II). (A) "Ligand fractionation model" as proposed by Beard et al. (*5*) and Johnson et al. (*12*), where Fe isotope fractionation is inferred to occur during the Fe redox change (Δ_1). Icopini et al. (*14*) alternatively propose that significant fractionation occurs during sorption of $Fe(II)_{aq}$ to the ferric substrate (Δ_2). In both models, ferric Fe in the substrate is not considered to be open to isotopic exchange with Fe(II) components, as marked by the figure in the lower right that illustrates zero % Fe^{3+} exchange in the substrate. (B) "Substrate redox cycling model", on the basis of the results of this study, which suggests that the Fe isotope composition of $Fe(II)_{aq}$ is controlled by isotopic exchange with a reactive Fe(III) pool ($Fe(III)_{reac}$) that lies in the outer layers of the ferric oxide substrate. Significant atom exchange is inferred to occur at the Fe(III) oxide surface, decreasing to zero % Fe^{3+} exchanged in the interior portions of iron oxide/hydroxide particles.

probably because of their ability to oxidize common fermentation products such as acetate and H_2 (*16*).

Methods

Bacterial Iron Oxide/Hydroxide Reduction Systems. The crystalline Fe(III) oxide phases goethite and hematite were employed in long-term (280 d) experiments with the dissimilatory iron-reducing bacterium *Geobacter sulfurreducens* (*36*, *37*). Because of their much lower specific surface area, crystalline phases such as goethite and hematite are subject to a much lower extent of enzymatic reduction compared to poorly crystalline Fe(III) oxide (*38*−*41*). As a result, microbial reduction of crystalline Fe(III) oxides generally leads to little or no production of secondary Fe(II)-bearing mineral precipitates such as magnetite (*42*−*46*), which is a common end product of poorly crystalline Fe(III) oxide reduction (*13*, *47*−*51*). Rather, Fe(II) generated during crystalline Fe(III) oxide reduction either remains in solution or becomes associated with residual Fe(III) oxide surfaces via surface complexation or surface precipitation reactions (*41*). The culture medium used was the simplest possible with no added phosphate, carbonate, sulfide, or organic carbon so as to minimize the likelihood of secondary Fe(II)-bearing mineral formation (cf. *13*). In addition, the long-term nature of our experiments was designed to maximize the likelihood that isotopic equilibrium would be achieved among the Fe pools that were open to isotopic exchange.

G. sulfurreducens cells were grown and collected as previously described (*52*). Batch experiments were carried out under nongrowth conditions (no added inorganic nutrients or vitamins) to minimize interactions between the media and ferric oxide/hydroxide phases. Hematite (8.0 g L^{-1}) or goethite (4.5 g L^{-1}) was added to 500 mL of Pipes buffer (10 mM, pH 6.8) in 1-L glass bottles equipped with a rubber stopper and sampling port with a thick butyl rubber septum. The media and headspace were bubbled with O_2-free H_2, which also served as the electron donor for the cells, and the bottles were crimp-sealed and autoclaved. Media was inoculated with an initial cell density of $\sim 10^8$ cells mL^{-1} and was incubated at 30 °C in the dark. This level of cell addition was chosen to maximize rate and extent of Fe(III) reduction of the well-crystallized substrates. Previous experiments have shown that under these conditions the amount of oxide surface limits Fe(III) reduction (*40*, *53*). All sampling was done in an anaerobic chamber using sterile needles and syringes.

Hematite powder (α-Fe_2O_3) was purchased from Fisher Scientific, whereas medium surface area (MSA) goethite was synthesized in the laboratory by neutralization of ferric chloride (54), and then was dried and passed through a 100-mesh sieve. Measured BET surface areas were ~ 10 m^2 g^{-1} (hematite) and ~ 55 m^2 g^{-1} (goethite). TEM analysis showed that hematite particles were spherical and ~100 nm in diameter, whereas goethite crystals were elongated and ~160 nm long by ~30 nm in diameter. X-ray diffraction and Mössbauer studies have shown that these synthetic Fe(III) oxides are free from major amorphous impurities (*40*, *42*, *46*, *55*). In addition, ascorbic acid dissolution studies indicate that the molar abundance of such impurities is very small (≤0.1%; *53*). These materials are also isotopically homogeneous, as discussed below.

Fe Phase Separation and Wet-Chemical Analysis. Over the course of the experiment, subsamples were taken from each culture and were separated into solid and aqueous fractions by centrifugation. The aqueous sample was passed through a 0.2-μm filter and was acidified with 6 M HCl. The solid portion was extracted for 1 h using a 1 M Na−acetate buffer (pH 4.85), which removed the majority of sorbed Fe(II) without dissolving the oxide substrate, on the basis of Fe(II) and Fe(III) concentration measurements. After the Na−acetate extraction, a second 1-h extraction was performed with 0.5 M HCl, which removed any remaining sorbed Fe(II) and partially dissolved the ferric oxide. Fe(II) and total Fe concentrations were determined using the *Ferrozine* reagent and NH_2OH−HCl (*56*), and Fe(III) concentrations were determined by difference. Fe concentration errors are based on the standard deviation of triplicate measurements, and errors for Fe(III) are calculated by the square root of the sum of the squares of Fe(II) and total Fe errors. Iron in the aqueous and Na−acetate fractions was almost exclusively Fe(II), whereas Fe(III) accounted for 8−42% (goethite) and 35−80% (hematite) of the total Fe in the 0.5 M HCl fraction.

Fe Isotope Measurements. Samples were purified for isotopic analysis using anion-exchange chromatography, followed by isotopic measurements using a multicollector, inductively coupled-plasma mass spectrometer (MC-ICP-MS), as previously described (*5*). All isotopic compositions are reported as δ^{56}Fe and δ^{57}Fe values, which reflect the $^{56}Fe/^{54}Fe$ and $^{57}Fe/^{54}Fe$ ratios, respectively, relative to the uniform baseline of terrestrial igneous rocks (*5*). External precision for δ^{56}Fe values is 0.05‰ (1σ), as determined by replicate analyses of 28 of the 76 samples reported in Tables 1−3 in the Supporting Information (abbreviated hereafter as SI). The initial δ^{56}Fe values of the hematite and goethite powders are +0.26‰ and +0.14‰, respectively. Successive partial dissolutions using 0.5 M HCl, as described in Johnson et al. (*12*), showed that isotopic compositions of the outer layers of the oxides were identical within error to the bulk composition, demonstrating that hematite and goethite were isotopically homogeneous prior to starting the experiments (Table 1, SI).

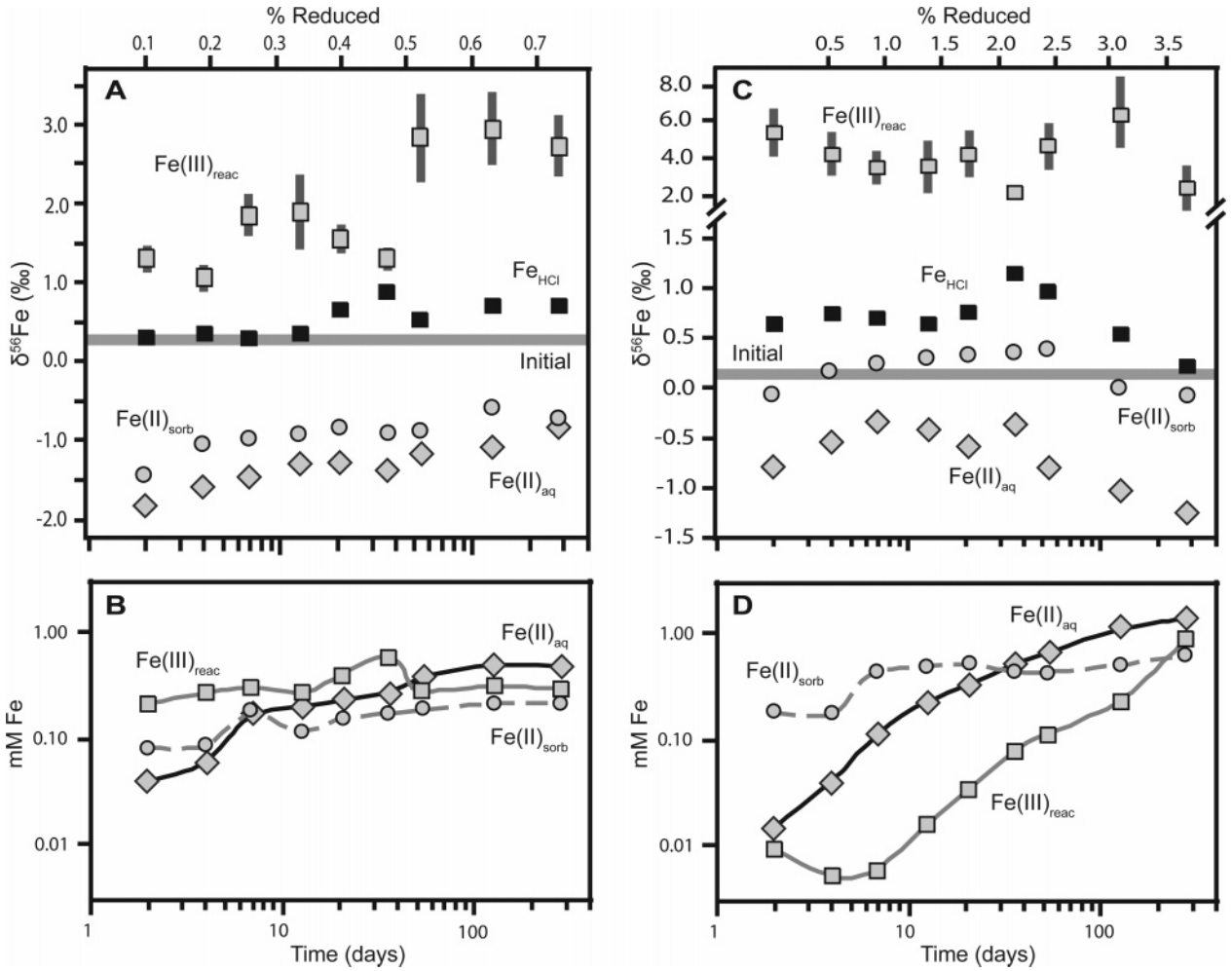

FIGURE 2. Measured δ^{56}Fe values and Fe concentrations for aqueous Fe(II), Na−acetate extractable (sorbed) Fe(II), and total Fe in the 0.5 M HCl extraction for the hematite (A and B) and goethite (C and D) experiments. Gray horizontal lines indicate the initial δ^{56}Fe values of the hematite and goethite. Gray squares with error bars show δ^{56}Fe values for reactive Fe(III) ($Fe(III)_{reac}$), which is the calculated isotopic composition of Fe(III) in the 0.5 M HCl extraction and is interpreted to represent Fe(III) at the oxide surface that is open to isotopic exchange. All other errors are smaller than the size of the symbols. The bottom scale shows the sampling day, and the top scale is the corresponding percent of starting Fe(III) reduced as calculated by regression of % Fe reduced-time relations (see Table 4 footnotes, SI).

Results

Isotopic Composition of Aqueous and Sorbed Fe(II). A key difference between this study and previous experiments on Fe isotope fractionation during DIR is that all components that were open to isotopic exchange were measured rather than simply comparing the isotopic composition of one product to the initial starting material. Aqueous and sorbed Fe(II) increased with time during hematite and goethite experiments (Figure 2B and 2D). Sorbed Fe(II), defined operationally as the sum of Fe(II) removed in the sequential Na−acetate and HCl extractions, initially comprised up to 65% (hematite) and 92% (goethite) of the total Fe(II) produced, whereas at the end of the experiment, the sorbed Fe(II) component approached ~30% of the total Fe(II) in both the hematite and goethite experiments. The Na−acetate extraction removed approximately 80% of the adsorbed Fe(II) in both hematite and goethite experiments, and the remaining sorbed Fe(II) was removed in the 0.5 M HCl treatment (Tables 2 and 3, SI).

In addition to tracing isotopic (atom) exchange, the temporal variation in Fe isotope compositions provides important constraints on the proportions of various Fe components that were open to isotopic exchange. As in previous experiments (*4*, *5*, *13*, *14*), δ^{56}Fe values for aqueous Fe(II) were 1.1−2.1‰ and 0.5−1.4‰ lower than the starting Fe(III) oxide material for hematite and goethite, respectively (Figure 2; Tables 2 and 3, SI). Isotopic mass balance requires a high-δ^{56}Fe component as the complement to the low-δ^{56}Fe values measured for aqueous (and sorbed) Fe(II). Because direct measurement of sorbed Fe(II) showed this component to have a δ^{56}Fe value less than or approximately equal to that of the initial substrate, in contrast to previous suggestions (*14*), this species cannot provide the required mass balance. In the hematite experiment, the isotopic fractionation between aqueous Fe(II) and sorbed Fe(II), defined as $\Delta_{Fe(II)aq-Fe(II)sorb}$, was −0.38‰ ± 0.10‰, and this remained constant over the 280-day experiment (Figure 3A). For the goethite experiment, the $\Delta_{Fe(II)aq-Fe(II)sorb}$ fractionation was −0.86‰ ± 0.17‰, and this also remained constant over the experiment (Figure 3C). Thus, in neither experiment was there evidence for the −2 to −5‰ $Fe(II)_{aq}$−$Fe(II)_{sorb}$ fractionations that were indirectly inferred by Icopini et al. (*14*), and a mechanism other than Fe(II) sorption is therefore required to explain the low-δ^{56}Fe values for $Fe(II)_{aq}$ produced during DIR.

Formation of a High ^{56}Fe/^{54}Fe Fe(III) Phase during DIR. At all time points during the experiments, the δ^{56}Fe values for Fe released via 0.5 M HCl extraction were equal to or higher than the starting Fe oxide material, with a maximum difference of 0.6‰ for hematite and 1.1‰ for goethite. The

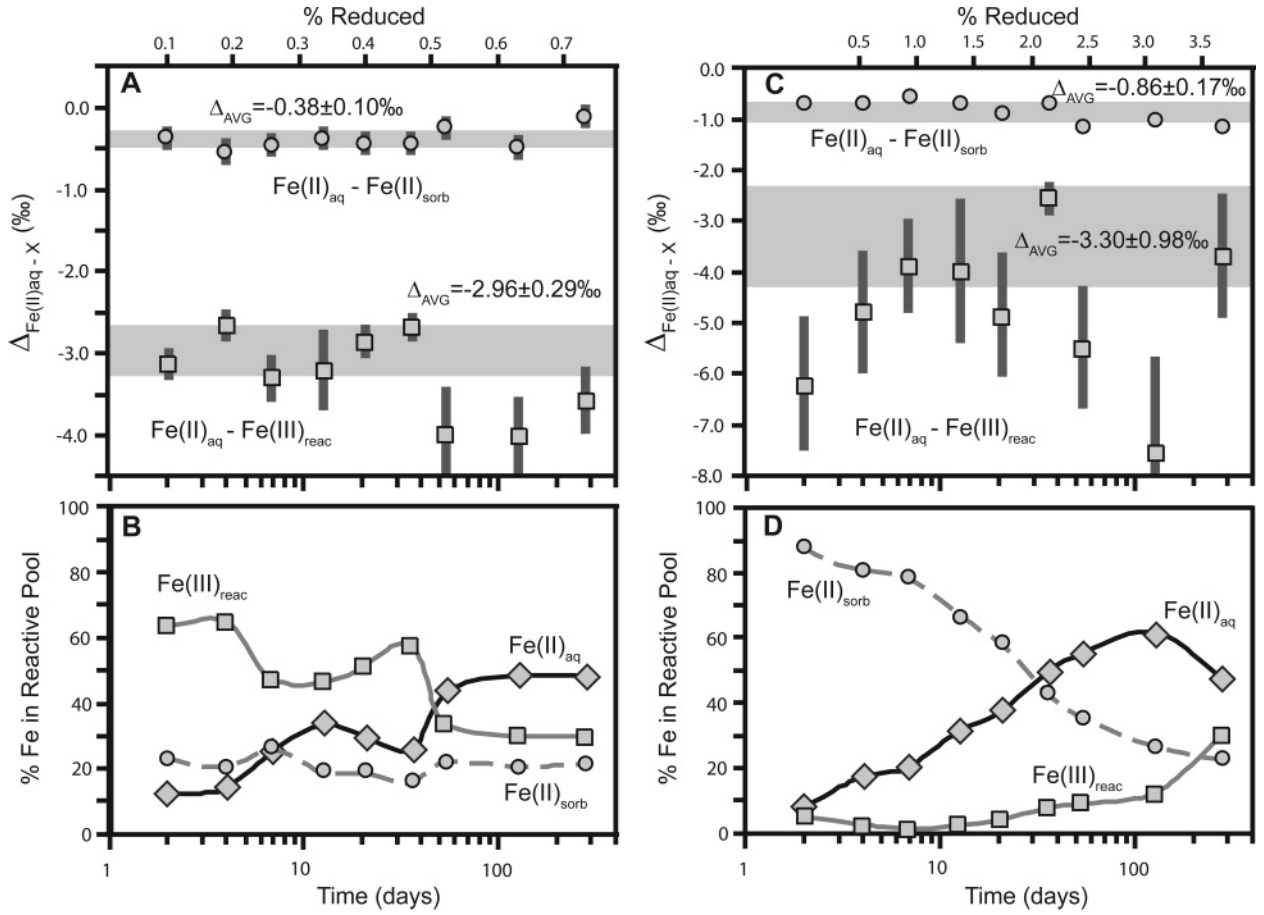

FIGURE 3. Calculated Fe isotope fractionation factors for $Fe(II)_{aq}-Fe(II)_{sorb}$ and $Fe(II)_{aq}-Fe(III)_{reac}$ and the % Fe these compounds comprise in the reactive Fe pool for the hematite (A and B) and goethite (C and D) experiments. Horizontal gray bars indicate weighted averages and 1σ uncertainties. The bottom scale shows the sampling day, and the top scale is the corresponding percent of Fe(III) reduced as calculated by regression of % Fe reduced-time relations (see Table 4 footnotes, SI).

0.5 M HCl extractions contained a mixture of Fe(II) and Fe(III) (Tables 2 and 3, SI), which is interpreted to reflect residual sorbed Fe(II) and dissolution of the outermost layers of the Fe(III) oxide surface. Preferential dissolution of smaller oxide particles is not a possibility, because TEM imaging showed goethite and hematite particles to be of reasonably uniform size before and after the 280-day experiment. Because δ^{56}Fe values of sorbed Fe(II) are rarely higher than the bulk Fe(III) oxide, and are generally significantly lower, the Fe(III) in the 0.5 M HCl extraction must have δ^{56}Fe values that are higher than the bulk Fe(III) oxide.

Precipitation of new phases at the oxide/hydroxide surface via oxidation of Fe(II) during sampling is unlikely, as the pO_2 in the anaerobic chamber was less than 10^{-6} atm (*57*), and the 40 mL of chamber atmosphere added to the bottles at each sampling (to maintain constant headspace pressure) corresponded to introduction of less than 0.1 μM of dissolved O_2. Batch experiments were carried out in media that contained no inorganic nutrients (NH_4^+ or PO_4^{3-}) and only low levels of dissolved inorganic carbon (<1 mM) to minimize the possibility of $FeCO_{3(s)}$ (siderite) or $Fe_3(PO_4)_{2(s)}$ (vivianite) precipitation, and no magnetite precipitation was observed by XRD or TEM analysis. Finally, the quantity of sorbed Fe(II) (Figure 2) and residual HCl-extractable Fe(II) (Tables 2 and 3, SI) remained relatively constant throughout the 280-day experiment, indicating no conversion of complexed Fe(II) at the oxide surface to magnetite. These considerations indicate that neither Fe(II) oxidation artifacts nor secondary Fe mineralization reactions can account for generation of high $^{56}Fe/^{54}Fe$ Fe(III) during hematite and goethite reduction.

The isotopic composition of the Fe(III) end member in the HCl extractions can be calculated from the proportions of Fe(II) and Fe(III) and the assumption that the Fe(II) component has a δ^{56}Fe value equal to that of the sorbed Fe(II) released in the Na−acetate wash. We refer to the Fe(III) component as "reactive Fe(III)" ($Fe(III)_{reac}$), because the shift in Fe isotope compositions indicates that this pool of Fe was open to isotopic (atom) exchange. The δ^{56}Fe value for $Fe(III)_{reac}$ in the HCl extraction may be calculated using the equation

$$\delta^{56}Fe_{HCl} = X^{HCl}_{Fe(II)}\delta^{56}Fe_{Fe(II)} + X^{HCl}_{Fe(III)reac}\delta^{56}Fe_{Fe(III)reac} \quad (1)$$

where $X^{HCl}_{Fe(Z)}$ is the mole fraction of each component. The δ^{56}Fe values for $Fe(III)_{reac}$ in the HCl extraction were calculated using the Excel add-in *Isoplot* (*58*), and uncertainties reflect error propagations on the basis of the Fe(II) fractions in the HCl extraction (Figures 2 and 3). Because Na−acetate extraction decreases the solution pH to levels below the sorption edge for Fe(II) (*59*), no isotopic fractionation of the sorbed Fe(II) component is expected during extraction, similar to dissolution of iron oxides with HCl (*60*). We will show below that the assumption that the δ^{56}Fe value of Fe(II) that was sampled in the 0.5 M HCl extraction is equal to that in the Na−acetate extraction is valid because of the consistency in calculated $Fe(II)_{aq}-Fe(III)_{reac}$ fractionation over a range in Fe(II) proportions in the HCl extraction.

The total $Fe(III)_{reac}$ component may be defined as the Fe(III) that is measured in the HCl extraction plus Fe(III) that was not sampled in the HCl extraction but is required

by isotopic mass balance constraints. In this system, the Fe isotope compositions of $Fe(II)_{aq}$, $Fe(II)_{sorb}$, and $Fe(III)_{reac}$, weighted by their relative proportions, must be equal to the Fe isotope compositions of the initial hematite or goethite. We therefore use a simple mass-balance equation to define the total $Fe(III)_{reac}$ pool as

$$M_{Fe(III)reac} = \frac{M_{Fe(II)aq}\delta^{56}Fe_{Fe(II)aq} + M_{Fe(II)sorb}\delta^{56}Fe_{Fe(II)sorb} - \delta^{56}Fe_{Fe(III)reac}(M_{Fe(II)aq} + M_{Fe(II)sorb})}{\delta^{56}Fe_{sys} - \delta^{56}Fe_{Fe(III)reac}} \quad (2)$$

where $M_{Fe(II)sorb}$ is the sum of Fe(II) in NaAc and HCl extractions, $\delta^{56}Fe_{Fe(II)sorb}$ is the $\delta^{56}Fe$ value of the NaAc extraction, $\delta^{56}Fe_{Fe(III)reac}$ is calculated from eq 1, $\delta^{56}Fe_{sys}$ is the Fe isotope composition of the total system (equal to the initial starting material), and all other quantities are measured as defined above.

The total $Fe(III)_{reac}$ pool is relatively constant with time in the hematite experiment (Figure 2B) but strongly increases with time in the goethite experiment (Figure 2D). The efficiency by which the HCl extraction sampled the $Fe(III)_{reac}$ component can be assessed by comparing the quantity of Fe(III) in the HCl extraction with the size of the total $Fe(III)_{reac}$ pool determined by isotopic mass balance, which indicates that the HCl extraction generally sampled 10−20% of the total $Fe(III)_{reac}$ pool in the hematite experiment (Table 4, SI), and a generally decreasing proportion with time in the goethite experiment (Table 4, SI), which broadly correlated with the increasing size of the total $Fe(III)_{reac}$ component with time (Figure 2D). Comparison of the total $Fe(III)_{reac}$ pool to initial amount of Fe(III) oxide material indicates that the reactive Fe(III) pool comprises less than 2% of the total Fe(III). This corresponds to a layer approximately one Fe(III) atom thick at the oxide surface, on the basis of average crystal size estimates from TEM images.

In many cases, the mole fraction of Fe(III) in the HCl extractions was quite low, with a mean of 0.15 for goethite and 0.53 for hematite. For samples where $X^{HCl}_{Fe(III)reac}$ was particularly low (e.g., 0.08−0.4), the corresponding errors for the calculated values of $\delta^{56}Fe_{Fe(III)reac}$ were high, because of larger extrapolation from the measured $\delta^{56}Fe_{HCl}$ value to the pure $\delta^{56}Fe_{Fe(III)reac}$ end member composition. Yet in all cases, calculated values for $\delta^{56}Fe_{Fe(III)reac}$ were substantially higher than the Fe oxide starting material. The weighted average of the fractionation factor between aqueous Fe(II) and reactive Fe(III) is -2.96 ± 0.29‰ for hematite and -3.30 ± 0.98‰ for goethite (Figure 3A and 3C; Table 4, SI). These values are remarkably similar to the experimentally determined equilibrium isotope fractionation factors between aqueous $[Fe(II)(H_2O)_6]^{2+}$ and hematite (*24*, *60*). At 22 °C, the equilibrium fractionation between $[Fe(II)(H_2O)_6]^{2+}$ and $[Fe(III)(H_2O)_6]^{3+}$ is -2.95 ± 0.38‰ (*24*), and the equilibrium fractionation between Fe(III) and hematite is ~ -0.1‰ at 98 °C, which is likely to be similar at 22 °C (*60*), producing an equilibrium $[Fe(II)(H_2O)_6]^{2+}$−Fe_2O_3 fractionation of −3.1‰ at 22 °C. We expect little isotopic difference between goethite and hematite because Fe is octahedrally coordinated in both minerals (*61*).

Discussion

Mechanism of Fe Isotope Fractionation during DIR. Our results provide new insights into the processes by which Fe isotopes may be fractionated during DIR. The results suggest that the major mechanism for Fe isotope fractionation is interfacial electron and Fe atom exchange between biogenic Fe(II) and Fe(III) oxide surface. This assertion is consistent with observations that the largest isotopic fractionations in transition metals occur between different redox states (*25*). Moreover, these results support a model similar to that proposed by Williams and Scherer (*26*) on the basis of Mössbauer spectroscopy, which documented electron exchange between sorbed Fe(II) and Fe(III) oxides in abiotic experiments.

The organism used in this study, *G. sulfurreducens*, is believed to require direct contact with the oxide surface for reduction to occur (*17*, *62*), so we assume that as Fe(II) is produced it will be associated with the oxide surface, either momentarily or perhaps longer if it remains adsorbed. During this time, Fe(II) may transfer electrons to the surface (e.g., $\equiv Fe^{III}OFe^{II} \rightarrow \equiv Fe^{II}OFe^{III}$; *29*), forming a layer of Fe(III) at the surface that resembles the underlying oxide (*26*) but is isotopically shifted to higher $^{56}Fe/^{54}Fe$ ratios through equilibrium isotope exchange. The fate of Fe(II) that participates in electron transfer is not clear, although some remains associated with the mineral surface (*26*), and our results indicate that the majority exists as either adsorbed or aqueous Fe(II). The total Fe(II) inventory has lower $^{56}Fe/^{54}Fe$ ratios than the cycled Fe(III) at the oxide surface, with minor isotopic partitioning within the ferrous Fe inventory between sorbed and aqueous Fe(II) ($\Delta_{Fe(II)aq-Fe(II)sorb}$), where slightly heavier Fe(II) remains adsorbed at the surface. The small differences in $Fe(II)_{aq}$−$Fe(II)_{sorb}$ fractionations between goethite and hematite in our experiments may reflect bonding differences for sorbed Fe(II) for these two ferric oxide/hydroxides.

The observed $\Delta_{Fe(II)aq-Fe(II)sorb}$ fractionations remained relatively constant over the 280-day experiments, which most likely reflects equilibrium isotope partitioning given the length of the experiment. In previous DIR experiments using poorly crystalline Fe(III) oxide (ferrihydrite) as the terminal electron acceptor, nonequilibrium isotope fractionations were believed to occur between sorbed and aqueous Fe(II) during the early stages of the experiments (*13*). Nonequilibrium effects may have occurred in the sorption experiments of Icopini et al. (*14*), where aqueous Fe(II) and goethite were instantaneously mixed and were allowed to sit for only 24 h prior to collection of samples for Fe isotope analysis. Alternatively, if interfacial electron/Fe atom exchange reactions and associated Fe isotope fractionation are rapid (e.g., time scale of minutes to hours), then equilibrium fractionation between aqueous Fe(II) and $Fe(III)_{reac}$ may have also contributed (at least in part) to the Fe isotope fractionations observed in these previous experiments.

Previous work by Icopini et al. (*14*) showed that during sorption of Fe(II) to goethite the remaining aqueous Fe(II) was ~0.8‰ lighter than the initial added Fe(II) solution after 24 h, which is comparable to the −0.93‰ fractionation between aqueous Fe(II) and goethite measured after 48 h in our biological experiments. Icopini et al. did not measure the isotopic composition of sorbed Fe(II) but rather assumed that the isotopic shift in aqueous Fe(II) was caused entirely by preferential sorption of heavy Fe(II) and then calculated the fractionation between aqueous and sorbed Fe(II). After 48 h in our goethite experiment, the measured $\Delta_{Fe(II)aq-Fe(II)sorb}$ fractionation was −0.72‰, much less than their calculated −2 to −5‰ fractionation (*14*). This suggests that the high-$\delta^{56}Fe$ component that Icopini et al. (*14*) inferred to be sorbed Fe(II) may have been $Fe(III)_{reac}$; indeed, Icopini et al. speculated that isotope exchange between ferric Fe in goethite and Fe(II) might be another explanation for their results. The mechanism proposed here for isotope fractionation during DIR requires interaction between Fe(II) and Fe(III) oxide surfaces for Fe isotope fractionation to occur, rather than simple Fe(II) adsorption, which is consistent with the observations of Icopini et al. (*14*) that no isotopic shift occurred when Fe(II) adsorbed to cell surfaces in the absence of iron oxides.

Environmental Implications. Our findings demonstrate that Fe isotopes record aqueous/solid-phase Fe redox cycling during DIR. Such redox cycling is likely to have a major impact

on surface reactivity in bacterial−mineral systems. For example, there has been considerable uncertainty and debate regarding the geochemical (e.g., thermodynamic and surface chemical) and microbiological factors that limit the extent of enzymatic reduction of crystalline Fe(III) oxides such as goethite and hematite (*3*, *16*, *41*, *63*−*65*), which are abundant in a wide variety of soils and sediments (*61*) and could thus be important substrates for DIR. It has been suggested that electron transfer between biogenic Fe(II) and residual Fe(III) oxide surfaces, leading to a mixed Fe(III)−Fe(II) surface phase (*29*, *31*), could impose a thermodynamic limitation on the extent of oxide reduction (*41*). The results reported here, together with recent spectroscopic evidence (*26*), provide conclusive evidence that such electron transfer occurs.

It is as yet unknown whether isotopic fractionations comparable to those observed in our DIR systems occur in abiologic systems in which $Fe(II)_{aq}$ contacts ferric oxides/hydroxides, nor are the kinetics of isotopic exchange in such systems known. In addition, it will be important to determine if the mechanism of isotopic fractionation determined here operates at greater extents of reduction (as is common for poorly crystalline Fe(III) oxides), or if it changes because of intrinsic limitations on the size of the reactive Fe(III) pool, particularly during transformation to minerals such as magnetite or other mixed Fe(II)−Fe(III) hydroxy phases (*13*, *49*, *66*). These are key issues that bear on application of Fe isotopes to tracing DIR in modern or ancient environments. If, for example, redox cycling in an abiotic $Fe(II)_{aq}$−ferric oxide system is limited to the outermost layers of the ferric oxide, significant quantities of low-δ^{56}Fe aqueous Fe(II) may be difficult to produce, and the very large inventory of low-δ^{56}Fe iron in Fe-rich sedimentary rocks may be best explained by biological processing of Fe (*11*, *13*).

Acknowledgments

We wish to thank G. Scott at the University of Alabama for sampling assistance, H. Xu for help with TEM and XRD work, and K. Nealson and two anonymous reviewers for helpful comments on the manuscript. Funding was provided by NSF grant EAR-0106614 and NASA-Ames grant NCC 2-5449 to C.M.J. and B.L.B., an award to E.E.R. through a NASA Astrobiology Institute grant to Jill Banfield at University of California Berkeley, and a NSF graduate fellowship to H.A.C.

Supporting Information Available

Three tables containing concentration and isotope measurements and a fourth table showing calculated fractionation factors. This material is available free of charge via the Internet at http://pubs.acs.org.

Literature Cited

(1) Nealson, K.; Saffarini, D. Iron and manganese in anaerobic respiration: environmental significance, physiology, and regulation. *Annu. Rev. Microbiol.* **1994**, *48*, 311−343.

(2) Vargas, M.; Kashefi, K.; Blunt-Harris, E.; Lovley, D. Microbiological evidence for Fe(III) reduction on early Earth. *Nature* **1998**, *395*, 65−67.

(3) Lovley, D. R. Fe(III) and Mn(IV) Reduction. In *Environmental Microbe-Metal Interactions*; Lovley, D. R., Ed.; ASM Press: Washington, DC, 2000; pp 3−30.

(4) Beard, B.; Johnson, C.; Cox, L.; Sun, H.; Nealson, K.; Aguilar, C. Iron isotope biosignatures. *Science* **1999**, *285*, 1889−1892.

(5) Beard, B.; Johnson, C.; Skulan, J.; Nealson, K.; Cox, L.; Sun, H. Application of Fe isotopes to tracing the geochemical and biological cycling of Fe. *Chem. Geol.* **2003**, *195*, 87−117.

(6) Brantley, S.; Liermann, L.; Bullen, T. Fractionation of Fe isotopes by soil microbes and organic acids. *Geology* **2001**, *29*, 535−538.

(7) Brantley, S.; Liermann, L.; Guynn, R.; Anbar, A.; Icopini, G.; Barling, J. Fe isotopic fractionation during mineral dissolution with and without bacteria. *Geochim. Cosmochim. Acta* **2004**, *68*, 3189−3204.

(8) Fantle, M. S.; DePaolo, D. J. Iron isotopic fractionation during continental weathering. *Earth Planet. Sci. Lett.* **2004**, *228*, 547.

(9) Severmann, S.; Johnson, C.; Beard, B.; McManus, J. The effect of early diagenesis on the Fe isotope compositions of porewaters and authigenic minerals in continental margin sediments. *Geochim. Cosmochim. Acta*, in revision.

(10) Johnson, C.; Beard, B.; Beukes, N.; Klein, C.; O'Leary, J. Ancient geochemical cycling in the Earth as inferred from Fe isotope studies of banded iron formations from the Transvaal Craton. *Contrib. Mineral. Petrol.* **2003**, *144*, 523−547.

(11) Yamaguchi, K.; Johnson, C.; Beard, B.; Ohmoto, H. Biogeochemical cycling of iron in the Archean-Paleoproterozoic Earth: Constraints from iron isotope variations in sedimentary rocks from the Kaapvaal and Pilbara Cratons. *Chem. Geol.* **2005**, *218*, 135−169.

(12) Johnson, C.; Beard, B.; Roden, E.; Newman, D.; Nealson, K. Isotopic constraints on biogeochemical cycling of Fe. *Rev. Mineral. Geochem.* **2004**, *55*, 359−408.

(13) Johnson, C.; Roden, E.; Welch, S.; Beard, B. Experimental constraints on Fe isotope fractionation during magnetite and Fe carbonate formation coupled to dissimilatory hydrous ferric oxide reduction. *Geochim. Cosmochim. Acta* **2005**, *69*, 963−993.

(14) Icopini, G.; Anbar, A.; Ruebush, S.; Tien, M.; Brantley, S. Iron isotope fractionation during microbial reduction of iron: The importance of adsorption. *Geology* **2004**, *32*, 205−208.

(15) Bullen, T.; White, A.; Childs, C.; Vivit, D.; Schulz, M. Demonstration of significant abiotic iron isotope fractionation in nature. *Geology* **2001**, *29*, 699−702.

(16) Lovley, D. R.; Holmes, D. E.; Nevin, K. Dissimilatory Fe(III) and Mn(IV) reduction. *Adv. Microb. Physiol.* **2004**; *49*, 219−286.

(17) Nevin, K.; Lovley, D. Mechanisms for Fe(III) oxide reduction in sedimentary environments. *Geomicrobiol. J.* **2002**, *19*, 141−159.

(18) Nevin, K.; Lovley, D. Mechanisms for accessing insoluble Fe(III) oxide during dissimilatory Fe(III) reduction by Geothrix fermentans. *Appl. Environ. Microbiol.* **2002**, *68*, 2294−2299.

(19) Rosso, K.; Zachara, J.; Fredrickson, J.; Gorby, Y.; Smith, S. Nonlocal bacterial electron transfer to hematite surfaces. *Geochim. Cosmochim. Acta* **2003**, *67*, 1081−1087.

(20) Newman, D.; Kolter, R. A role for excreted quinones in extracellular electron transfer. *Nature* **2000**, *405*, 94−97.

(21) Canfield, D. Biogeochemistry of sulfur isotopes. *Rev. Mineral. Geochem.* **2001**, *43*, 607−636.

(22) Bruchert, V. Physiological and ecological aspects of sulfur isotope fractionation during bacterial sulfate reduction. In *Sulfur Biogeochemistry - Past and Present: GSA Special Paper*; Amend, J., Edwards, K., Lyons, T., Eds., The Geological Society of America: Boulder, CO, 2004; Vol. 379, pp 1−16.

(23) Johnson, C.; Skulan, J.; Beard, B.; Sun, H.; Nealson, K.; Braterman, P. Isotopic fractionation between Fe(III) and Fe(II) in aqueous solutions. *Earth Planet. Sci. Lett.* **2002**, *195*, 141−153.

(24) Welch, S.; Beard, B.; Johnson, C.; Braterman, P. Kinetic and equilibrium Fe isotope fractionation between aqueous Fe(II) and Fe(III). *Geochim. Cosmochim. Acta* **2003**, *67*, 4231−4250.

(25) Schauble, E. Applying stable isotope fractionation theory to new systems. *Rev. Mineral. Geochem.* **2004**, *55*, 65−111.

(26) Williams, A.; Scherer, M. Spectroscopic evidence for Fe(II)-Fe(III) electron transfer at the iron oxide-water interface. *Environ. Sci. Technol.* **2004**, *38*, 4782−4790.

(27) Tronc, E.; Belleville, P.; Jolivet, J.; Livage, J. Transformation of ferric hydroxide into spinel by Fe(II) adsorption. *Langmuir* **1992**, *8*, 313−319.

(28) Jeon, B.; Dempsey, B.; Burgos, W. Kinetics and mechanisms for reactions of Fe(II) with iron(III) oxides. *Environ. Sci. Technol.* **2003**, *37*, 3309−3315.

(29) Coughlin, B.; Stone, A. Nonreversible adsorption of divalent metal ions (Mn-II, Co-II, Ni-II, Cu-II, and Pb-II) onto goethite: effects of acidification, Fe-II addition, and picolinic acid addition. *Environ. Sci. Technol.* **1995**, *29*, 2445−2455.

(30) Pecher, K.; Haderlein, S.; Schwarzenbach, R. Reduction of polyhalogenated methanes by surface-bound Fe(II) in aqueous suspensions of iron oxides. *Environ. Sci. Technol.* **2002**, *36*, 1734−1741.

(31) Sherman, D. Molecular orbital (SCF-X-ALPHA-SW) theory of metal-metal charge transfer processes in minerals 1. Application to Fe-2+ to Fe-3+ charge transfer and "electron delocalization" in mixed-valence iron oxides and silicates. *Phys. Chem. Miner.* **1987**, *14*, 355−363.

(32) Jolivet, J.; Tronc, E.; Barbe, C.; Livage, J. Interfacial electron-transfer in colloidal spinel iron oxide silver ion reduction in aqueous medium. *J. Colloid Interface Sci.* **1990**, *138*, 465−472.

(33) Roling, W. F. M.; van Breukelen, B. M.; Braster, M.; Lin, B.; van Verseveld, H. W. Relationships between microbial community structure and hydrochemistry in a landfill leachate-polluted aquifer. *Appl. Environ. Microbiol.* **2001**, *67*, 4619−4629.
(34) Stein, L.; La Duc, M.; Grundl, T.; Nealson, K. Bacterial and archaeal populations associated with freshwater ferromanganous micronodules and sediments. *Environ. Microbiol.* **2001**, *3*, 10−18.
(35) Anderson, R. T.; Vrionis, H. A.; Ortiz-Bernad, I.; Resch, C. T.; Long, P. E.; Dayvault, R.; Karp, K.; Marutzky, S.; Metzler, D. R.; Peacock, A.; White, D. C.; Lowe, M.; Lovley, D. R. Stimulating the in situ activity of Geobacter species to remove uranium from the groundwater of a uranium-contaminated aquifer. *Appl. Environ. Microbiol.* **2003**, *69*, 5884−5891.
(36) Caccavo, F.; Blakemore, R.; Lovley, D. A hydrogen-oxidizing, Fe(III)-reducing microorganism from the Great Bay Estuary, New Hampshire. *Appl. Environ. Microbiol.* **1992**, *58*, 3211−3216.
(37) Methe, B.; Nelson, K.; Eisen, J.; Paulsen, I.; Nelson, W.; Heidelberg, J.; Wu, D.; Wu, M.; Ward, N.; Beanan, M.; Dodson, R.; Madupu, R.; Brinkac, L.; Daugherty, S.; DeBoy, R.; Durkin, A.; Gwinn, M.; Kolonay, J.; Sullivan, S.; Haft, D.; Selengut, J.; Davidsen, T.; Zafar, N.; White, O.; Tran, B.; Romero, C.; Forberger, H.; Weidman, J.; Khouri, H.; Feldblyum, T.; Utterback, T.; Van Aken, S.; Lovley, D.; Fraser, C. Genome of Geobacter sulfurreducens: Metal reduction in subsurface environments. *Science* **2003**, *302*, 1967−1969.
(38) Lovley, D.; Phillips, E. Availability of ferric iron for microbial reduction in bottom sediments of the freshwater tidal Potomac River. *Appl. Environ. Microbiol.* **1986**, *52*, 751−757.
(39) Lovley, D.; Phillips, E. Novel mode of microbial energy metabolism: organic carbon oxidation coupled to dissimilatory reduction of iron or manganese. *Appl. Environ. Microbiol.* **1988**, *54*, 1472−1480.
(40) Roden, E.; Zachara, J. Microbial reduction of crystalline iron(III) oxides: Influence of oxide surface area and potential for cell growth. *Environ. Sci. Technol.* **1996**, *30*, 1618−1628.
(41) Roden, E.; Urrutia, M. Influence of biogenic Fe(II) on bacterial crystalline Fe(III) oxide reduction. *Geomicrobiol. J.* **2002**, *19*, 209−251.
(42) Zachara, J.; Fredrickson, J.; Li, S.; Kennedy, D.; Smith, S.; Gassman, P. Bacterial reduction of crystalline Fe^{3+} oxides in single phase suspensions and subsurface materials. *Am. Mineral.* **1998**, *83*, 1426−1443.
(43) Fredrickson, J.; Zachara, J.; Kennedy, D.; Duff, M.; Gorby, Y.; Li, S.; Krupka, K. Reduction of U(VI) in goethite (alpha-FeOOH) suspensions by a dissimilatory metal-reducing bacterium. *Geochim. Cosmochim. Acta* **2000**, *64*, 3085−3098.
(44) Zachara, J.; Fredrickson, J.; Smith, S.; Gassman, P. Solubilization of Fe(III) oxide-bound trace metals by a dissimilatory Fe(III) reducing bacterium. *Geochim. Cosmochim. Acta* **2001**, *65*, 75−93.
(45) Kukkadapu, R.; Zachara, J.; Smith, S.; Fredrickson, J.; Liu, C. Dissimilatory bacterial reduction of Al-substituted goethite in subsurface sediments. *Geochim. Cosmochim. Acta* **2001**, *65*, 2913−2924.
(46) Weber, K.; Churchill, M.; Urrutia, M.; Kukkadapu, R.; Roden, E. Anaerobic redox cycling of iron by freshwater sediment microorganisms. *Environ. Microbiol.*, in press.
(47) Lovley, D.; Stolz, J.; Nord, G.; Phillips, E. Anaerobic production of magnetite by a dissimilatory iron-reducing microorganism. *Nature* **1987**, *330*, 252−254.
(48) Roden, E.; Lovley, D. Dissimilatory Fe(III) reduction by the marine microorganism desulfuromonas acetoxidans. *Appl. Environ. Microbiol.* **1993**, *59*, 734−742.
(49) Fredrickson, J.; Zachara, J.; Kennedy, D.; Dong, H.; Onstott, T.; Hinman, N.; Li, S. Biogenic iron mineralization accompanying the dissimilatory reduction of hydrous ferric oxide by a groundwater bacterium. *Geochim. Cosmochim. Acta* **1998**, *62*, 3239−3257.
(50) Zachara, J.; Kukkadapu, R.; Fredrickson, J.; Gorby, Y.; Smith, S. Biomineralization of poorly crystalline Fe(III) oxides by dissimilatory metal reducing bacteria (DMRB). *Geomicrobiol. J.* **2002**, *19*, 179−207.
(51) Hansel, C.; Benner, S.; Nico, P.; Fendorf, S. Structural constraints of ferric (hydr)oxides on dissimilatory iron reduction and the fate of Fe(II). *Geochim. Cosmochim. Acta* **2004**, *68*, 3217−3229.
(52) Jeon, B.; Kelly, S.; Kemner, K.; Barnett, M.; Burgos, W.; Dempsey, B.; Roden, E., Microbial reduction of U(VI) at the solid-water interface. *Environ. Sci. Technol.* **2004**, *38*, 5649−5655.
(53) Roden, E. Geochemical and microbiological controls on dissimilatory iron reduction. *C. R. Geosci.*, submitted.
(54) Schwertmann, U.; Cornell, R. M. *Iron Oxides in the Laboratory*; VCH: New York, 1991.
(55) Jeon, B.; Dempsey, B.; Burgos, W.; Royer, R. Reactions of ferrous iron with hematite. *Colloids Surf., A* **2001**, *191*, 41−55.
(56) Stookey, L. Ferrozine: A new spectrophotometric reagent for iron. *Anal. Chem.* **1970**, *42*, 779−781.
(57) Jeon, B.; Dempsey, B.; Royer, R.; Burgos, W. Low-temperature oxygen trap for maintaining strict anoxic conditions. *J. Environ. Eng. (Am. Soc. Civ. Eng.)* **2004**, *130*, 1407−1410.
(58) Ludwig, K. R. *ISOPLOT.; a plotting and regression program for radiogenic-isotope data,* version 2.53; U.S. Geological Survey: Reston, VA, 1991.
(59) Liger, E.; Charlet, L.; Van Cappellen, P. Surface catalysis of uranium(VI) reduction by iron(II). *Geochim. Cosmochim. Acta* **1999**, *63*, 2939−2955.
(60) Skulan, J.; Beard, B.; Johnson, C. Kinetic and equilibrium Fe isotope fractionation between aqueous Fe(III) and hematite. *Geochim. Cosmochim. Acta* **2002**, *66*, 2995−3015.
(61) Cornell, R. M.; Schwertmann, U. *The Iron Oxides: Structure, Properties, Reactions, Occurrences and Uses*, 2nd ed.; VCH: New York, 2003.
(62) Nevin, K.; Lovley, D. Lack of production of electron-shuttling compounds or solubilization of Fe(III) during reduction of insoluble Fe(III) oxide by Geobacter metallireducens. *Appl. Environ. Microbiol.* **2000**, *66*, 2248−2251.
(63) Liu, C.; Zachara, J.; Gorby, Y.; Szecsody, J.; Brown, C. Microbial reduction of Fe(III) and sorption/precipitation of Fe(II) on Shewanella putrefaciens strain CN32. *Environ. Sci. Technol.* **2001**, *35*, 1385−1393.
(64) Roden, E.; Urrutia, M. Ferrous iron removal promotes microbial reduction of crystalline iron(III) oxides. *Environ. Sci. Technol.* **1999**, *33*, 1847−1853.
(65) Royer, R.; Dempsey, B.; Jeon, B.; Burgos, W. Inhibition of biological reductive dissolution of hematite by ferrous iron. *Environ. Sci. Technol.* **2004**, *38*, 187−193.
(66) Hansel, C.; Benner, S.; Neiss, J.; Dohnalkova, A.; Kukkadapu, R.; Fendorf, S. Secondary mineralization pathways induced by dissimilatory iron reduction of ferrihydrite under advective flow. *Geochim. Cosmochim. Acta* **2003**, *67*, 2977−2992.

Received for review March 18, 2005. Revised manuscript received June 16, 2005. Accepted June 19, 2005.

ES0505346

Supporting Information

Coupled Fe(II)-Fe(III) electron and atom exchange as a mechanism for Fe isotope fractionation during dissimilatory iron oxide reduction

Heidi A. Crosby, Clark M. Johnson, Eric E. Roden, Brian L. Beard

4 pages

4 tables

Table 1. Initial Fe isotope compositions of ferric oxide starting materials and tests for isotopic homogeneity.

Sample	Aliquot[a]	Analyses				Average of Replicates			
		δ^{56}Fe	2-SE[b]	δ^{57}Fe	2-SE	δ^{56}Fe	1-SD[c]	δ^{57}Fe	1-SD
Hematite starting material									
	1	0.22	0.06	0.36	0.03	0.26	0.04	0.40	0.05
	repeat	0.29	0.04	0.41	0.04				
	2	0.29	0.07	0.40	0.03				
	repeat	0.31	0.06	0.48	0.03				
	3	0.22	0.05	0.42	0.05				
	4	0.23	0.03	0.34	0.03				
Hematite partial dissolutions									
2.0 % dissolved, aqueous		0.35	0.04	0.54	0.03				
2.0 % dissolved, solids		0.15	0.04	0.26	0.03				
4.7 % dissolved, aqueous		0.28	0.05	0.41	0.03				
4.7 % dissolved, solids		0.16	0.03	0.30	0.03				
11.1 % dissolved, aqueous		0.22	0.04	0.23	0.09				
11.1% dissolved, solids		0.08	0.03	0.20	0.03				
21.1 % dissolved, aqueous		0.19	0.07	0.21	0.04				
21.1 % dissolved, solids		0.16	0.04	0.26	0.04				
45.4 % dissolved, aqueous		0.34	0.05	0.48	0.03				
45.4 % dissolved, solids		0.23	0.02	0.34	0.02				
Goethite starting material									
	1	0.10	0.04	0.14	0.03	0.14	0.06	0.21	0.10
	repeat	0.15	0.07	0.23	0.04				
	2	0.24	0.07	0.35	0.06				
	3	0.16	0.03	0.25	0.04				
	4	0.07	0.02	0.09	0.03				
Goethite partial dissolutions									
0.7 % dissolved, aqueous		-0.01	0.03	-0.03	0.03				
0.7 % dissolved, solids		0.14	0.03	0.22	0.05				
1.2 % dissolved, aqueous		-0.03	0.03	-0.05	0.03				
1.2 % dissolved, solids		0.06	0.04	0.08	0.03				
2.0 % dissolved, aqueous		0.08	0.05	0.10	0.03				
2.0 % dissolved, solids		0.09	0.03	0.18	0.03				
3.9 % dissolved, aqueous		0.18	0.03	0.29	0.03				
3.9 % dissolved, solids		0.10	0.03	0.15	0.03				
9.5 % dissolved, aqueous		0.21	0.03	030	0.02				
9.5 % dissolved, solids		0.23	0.03	0.33	0.03				

[a] Different aliquots are from the same sample but separately processed through anion-exchange chromatography, whereas repeats are different isotopic analyses of the same aliquot.
[b] 2-SE is the internal standard error based on 40 10-second on peak integrations taken for each analysis.
[c] 1-SD is the standard deviation of multiple measurements of the same sample (either repeats of one aliquot or different aliquots processed separately through anion exchange chromatography).

Table 2. Fe isotope compositions of aqueous, Na-acetate (NaAc) and 0.5M HCl (HCl) fractions for *G. sulfurreducens* reduction of hematite.

Sample	Aliquot	Day	Fe(II)	error[a]	Fe(III)	error	Analyses[b]				Average of Replicates			
			(mM)	(mM)	(mM)	(mM)	δ^{56}Fe	2-SE	δ^{57}Fe	2-SE	δ^{56}Fe	1-SD	δ^{57}Fe	1-SD
Aqueous		0.00	0.001	0.0022	0.000	0.0032								
NaAc		0.00	0.000	0.0000	0.000	0.0000								
HCl		0.00	0.000	0.0000	0.000	0.0000								
Aqueous	1	2.00	0.041	0.0022	0.000	0.0032	-1.81	0.05	-2.68	0.04	-1.83	0.03	-2.67	0.01
	repeat						-1.85	0.06	-2.66	0.03				
NaAc	1	2.00	0.060	0.0010	0.000	0.0018	-1.52	0.07	-2.19	0.03	-1.46	0.09	-2.12	0.10
	2						-1.40	0.03	-2.06	0.02				
HCl	1	2.00	0.017	0.0000	0.031	0.0000	0.34	0.04	0.42	0.05	0.30	0.05	0.44	0.02
	2						0.27	0.03	0.45	0.02				
Aqueous	1	4.00	0.059	0.0022	0.000	0.0032	-1.59	0.03	-2.34	0.03				
NaAc	1	4.00	0.065	0.0022	0.001	0.0027	-1.06	0.03	-1.47	0.03				
HCl	1	4.00	0.019	0.0000	0.038	0.0012	0.34	0.03	0.44	0.03	0.35	0.01	0.51	0.09
	2						0.35	0.03	0.57	0.02				
Aqueous	1	6.83	0.163	0.0022	0.041	0.0022	-1.46	0.03	-2.14	0.02	-1.45	0.02	-2.12	0.04
	repeat						-1.44	0.03	-2.09	0.04				
NaAc	1	6.83	0.132	0.0039	0.004	0.0044	-1.07	0.02	-1.61	0.03	-1.00	0.10	-1.51	0.14
	repeat						-0.94	0.07	-1.41	0.05				
HCl	1	6.83	0.037	0.0010	0.030	0.0018	0.39	0.04	0.53	0.03	0.30	0.12	0.37	0.23
	repeat						0.21	0.06	0.21	0.06				
Aqueous	1	12.7	0.196	0.0077	0.024	0.0104	-1.23	0.04	-1.86	0.04	-1.30	0.11	-1.93	0.11
	2						-1.38	0.06	-2.01	0.04				
NaAc	1	12.7	0.087	0.0092	0.003	0.0127	-0.91	0.03	-1.36	0.04	-0.93	0.03	-1.33	0.05
	2						-0.96	0.03	-1.30	0.03				
HCl	1	12.7	0.025	0.0029	0.021	0.0055	0.35	0.03	0.56	0.03	0.33	0.12	0.51	0.18
	2						0.21	0.03	0.30	0.03				
	repeat						0.45	0.04	0.66	0.03				
Aqueous	1	20.7	0.233	0.0022	0.018	0.0052	-1.32	0.09	-1.93	0.04	-1.29	0.04	-1.92	0.02
	repeat						-1.27	0.03	-1.91	0.03				
NaAc	1	20.7	0.123	0.0006	0.009	0.0030	-0.83	0.03	-1.18	0.03	-0.86	0.04	-1.22	0.07
	2						-0.89	0.05	-1.27	0.02				
HCl	1	20.7	0.025	0.0006	0.039	0.0008	0.57	0.06	0.79	0.03	0.63	0.05	0.91	0.11
	2						0.67	0.03	0.99	0.03				
	repeat						0.64	0.04	0.95	0.04				
Aqueous	1	35.8	0.265	0.0000	0.014	0.0047	-1.36	0.09	-2.02	0.04				
NaAc	1	35.8	0.135	0.0006	0.010	0.0013	-0.90	0.04	-1.27	0.05	-0.93	0.04	-1.37	0.13
	2						-0.96	0.03	-1.46	0.03				
HCl	1	35.8	0.030	0.0010	0.118	0.0011	0.94	0.04	1.40	0.04	0.86	0.07	1.25	0.13
	2						0.80	0.03	1.15	0.03				
	repeat						0.84	0.04	1.21	0.05				
Aqueous	1	53.7	0.372	0.0138	0.018	0.0207	-1.17	0.07	-1.76	0.06	-1.15	0.02	-1.78	0.04
	2						-1.14	0.06	-1.81	0.04				
NaAc	1	53.7	0.155	0.0019	0.000	0.0030	-0.90	0.04	-1.34	0.03				
HCl	1	53.7	0.033	0.0025	0.020	0.0040	0.50	0.05	0.76	0.05				
Aqueous	1	127	0.496	0.0117	0.016	0.0194	-1.13	0.03	-1.67	0.03	-1.07	0.09	-1.57	0.14
	repeat						-1.00	0.03	-1.47	0.03				
NaAc	1	127	0.182	0.0029	0.024	0.0039	-0.50	0.03	-0.82	0.03	-0.59	0.07	-0.89	0.07
	repeat						-0.59	0.04	-0.84	0.04				
	2						-0.68	0.03	-0.97	0.03				
	repeat						-0.59	0.04	-0.92	0.04				
HCl	1	127	0.027	0.0015	0.015	0.0075	0.68	0.04	1.09	0.03	0.68	0.01	1.02	0.10
	2						0.68	0.06	0.95	0.05				
Aqueous	1	280	0.472	0.0077	0.050	0.0193	-0.84	0.03	-1.20	0.03				
NaAc	1	280	0.182	0.0031	0.006	0.0039	-0.74	0.03	-1.10	0.03				
HCl	1	280	0.031	0.0017	0.021	0.0034	0.67	0.03	0.95	0.04				

[a]Fe(II) and total Fe were measured using *Ferrozine*, and Fe(III) was determined by difference. Errors are based on the standard deviation of triplicate measurements, and errors for Fe(III) use the square root of the sum of the squares of Fe(II) and total Fe errors.
[b]Errors for isotopic measurements are described in Table 1, Supporting Information.

Table 3. Fe isotope compositions of aqueous, Na-acetate (NaAc) and 0.5M HCl (HCl) fractions for *G. sulfurreducens* reduction of goethite.

Sample	Aliquot	Day	Fe(II)	error	Fe(III)	error	Analyses				Average of Replicates			
			(mM)	(mM)	(mM)	(mM)	δ^{56}Fe	2-SE	δ^{57}Fe	2-SE	δ^{56}Fe	1-SD	δ^{57}Fe	1-SD
Aqueous		0.00	0.000	0.0000	0.000	0.0000								
NaAc		0.00	0.000	0.0000	0.000	0.0000								
HCl		0.00	0.000	0.0000	0.000	0.0000								
Aqueous	1	2.00	0.015	0.0000	0.000	0.0000	-0.79	0.03	-1.09	0.02				
NaAc	1	2.00	0.135	0.0040	0.001	0.0056	-0.07	0.03	-0.03	0.03				
HCl	1	2.00	0.042	0.0010	0.006	0.0018	0.65	0.03	0.96	0.03				
Aqueous	1	4.00	0.038	0.0000	0.001	0.0024	-0.54	0.04	-0.80	0.05				
NaAc	1	4.00	0.144	0.0000	0.000	0.0006	0.17	0.03	0.31	0.03				
HCl	1	4.00	0.032	0.0000	0.005	0.0000	0.67	0.03	1.05	0.03	0.73	0.08	1.07	0.03
	2						0.79	0.07	1.09	0.05				
Aqueous	1	6.83	0.113	0.0059	0.042	0.0071	-0.38	0.03	-0.57	0.03				
NaAc	1	6.83	0.349	0.0044	0.010	0.0060	0.23	0.06	0.40	0.03				
HCl	1	6.83	0.088	0.0006	0.015	0.0036	0.72	0.03	1.12	0.03	0.70	0.03	1.06	0.09
	2						0.68	0.04	1.00	0.05				
Aqueous	1	12.7	0.221	0.0044	0.034	0.0050	-0.41	0.08	-0.61	0.08				
NaAc	1	12.7	0.363	0.0115	0.013	0.0128	0.29	0.03	0.47	0.02				
HCl	1	12.7	0.102	0.0019	0.012	0.0025	0.63	0.03	0.93	0.02				
Aqueous	1	20.7	0.326	0.0038	0.024	0.0056	-0.58	0.06	-0.83	0.07				
NaAc	1	20.7	0.404	0.0011	0.006	0.0026	0.34	0.05	0.49	0.03	0.33	0.01	0.52	0.04
	2						0.32	0.03	0.54	0.03				
HCl	1	20.7	0.104	0.0006	0.013	0.0012	0.78	0.06	1.25	0.04	0.77	0.02	1.20	0.06
	2						0.75	0.02	1.16	0.02				
Aqueous	1	35.8	0.494	0.0080	0.026	0.0101	-0.37	0.03	-0.50	0.03				
NaAc	1	35.8	0.339	0.0028	0.027	0.0229	0.37	0.04	0.60	0.04				
HCl	1	35.8	0.097	0.0034	0.068	0.0035	1.16	0.07	1.86	0.05	1.11	0.07	1.79	0.10
	2						1.06	0.05	1.72	0.03				
Aqueous	1	53.7	0.654	0.0022	0.010	0.0046	-0.80	0.05	-1.20	0.04				
NaAc	1	53.7	0.344	0.0020	0.010	0.0020	0.38	0.03	0.58	0.03				
HCl	1	53.7	0.075	0.0022	0.012	0.0031	0.96	0.08	1.46	0.04				
Aqueous	1	127	1.145	0.0363	0.000	0.0378	-1.04	0.04	-1.55	0.03				
NaAc	1	127	0.390	0.0031	0.067	0.0069	-0.10	0.03	-0.18	0.02	-0.05	0.07	-0.11	0.10
	2						-0.01	0.02	-0.04	0.03				
HCl	1	127	0.098	0.0015	0.009	0.0034	0.59	0.06	0.92	0.05	0.52	0.07	0.78	0.01
	2						0.47	0.06	0.67	0.03				
	3						0.51	0.03	0.74	0.03				
Aqueous	1	280	1.366	0.0066	0.026	0.0316	-1.24	0.03	-1.70	0.04				
NaAc	1	280	0.538	0.0051	0.013	0.0114	-0.08	0.03	-0.10	0.03				
HCl	1	280	0.094	0.0020	0.013	0.0022	0.22	0.05	0.27	0.04				

Analysis methods and error calculations as in Tables 1 and 2, Supporting Information.

Table 4. Relative proportions of Fe species and calculated Fe isotope fractionations.

Day	Reduction rate % Fe(II)/d[a]	$\frac{Fe_{reac}}{Fe_{Tot}}$[b]	$\frac{Fe(II)_{aq}}{Fe_{reac}}$	$\frac{Fe(II)_{sorb}}{Fe_{reac}}$	$\frac{Fe(III)_{reac}}{Fe_{reac}}$	$\frac{Fe(III)^{meas}_{reac}}{Fe(III)_{reac}}$	$\Delta_{Fe(II)aq-Fe(II)sorb}$	error 2σ	$\Delta_{Fe(II)sorb-FO}$[c]	error 2σ	$\Delta_{Fe(II)aq Fe(III)reac}$	error 2σ[d]
Hematite experiment												
2.0	2.75×10^{-2}	0.0033	0.1253	0.2349	0.6398	0.1464	-0.37	0.14	-1.72	0.14	-3.13	0.19
4.0	2.51×10^{-2}	0.0042	0.1415	0.2023	0.6561	0.1375	-0.53	0.14	-1.32	0.14	-2.66	0.19
6.8	2.20×10^{-2}	0.0064	0.2549	0.2644	0.4807	0.0993	-0.45	0.14	-1.26	0.14	-3.31	0.28
12.7	1.68×10^{-2}	0.0058	0.3394	0.1941	0.4665	0.0765	-0.37	0.14	-1.19	0.14	-3.19	0.48
20.7	1.11×10^{-2}	0.0078	0.2976	0.1881	0.5143	0.0974	-0.43	0.14	-1.12	0.14	-2.86	0.20
35.8	5.83×10^{-3}	0.0102	0.2588	0.1607	0.5805	0.1992	-0.43	0.14	-1.19	0.14	-2.67	0.16
53.7	2.57×10^{-3}	0.0085	0.4380	0.2213	0.3407	0.0679	-0.25	0.14	-1.16	0.14	-3.98	0.57
126.7	9.08×10^{-5}	0.0102	0.4882	0.2057	0.3061	0.0490	-0.47	0.14	-0.85	0.14	-4.01	0.47
279.7	8.11×10^{-8}	0.0098	0.4816	0.2166	0.3018	0.0707	-0.10	0.14	-1.00	0.14	-3.57	0.40
Average:							**-0.38**	**0.10**			**-2.96**	**0.29**
Goethite experiment												
2.0	8.02×10^{-2}	0.0040	0.0758	0.8753	0.0489	0.6410	-0.72	0.14	-0.21	0.14	-6.21	1.30
4.0	7.66×10^{-2}	0.0044	0.1750	0.8007	0.0242	0.9431	-0.71	0.14	0.03	0.14	-4.79	1.20
6.8	7.18×10^{-2}	0.0111	0.2027	0.7867	0.0105	~1.0	-0.58	0.14	0.08	0.14	-3.89	0.92
12.7	6.28×10^{-2}	0.0140	0.3151	0.6621	0.0228	0.7328	-0.70	0.14	0.15	0.14	-3.99	1.40
20.7	5.12×10^{-2}	0.0174	0.3757	0.5857	0.0386	0.3848	-0.91	0.14	0.19	0.14	-4.85	1.20
35.8	3.71×10^{-2}	0.0202	0.4891	0.4315	0.0794	0.8543	-0.72	0.14	0.20	0.14	-2.56	0.31
53.7	2.47×10^{-2}	0.0237	0.5512	0.3533	0.0956	0.1038	-1.18	0.14	0.24	0.14	-5.49	1.20
126.7	4.67×10^{-3}	0.0371	0.6166	0.2625	0.1209	0.0389	-1.02	0.14	-0.16	0.14	-7.57	1.90
279.7	1.42×10^{-4}	0.0576	0.4740	0.2195	0.3065	0.0143	-1.16	0.14	-0.22	0.14	-3.69	1.20
Average:							**-0.86**	**0.17**			**-3.30**	**0.98**

[a]Rate of Fe reduction, in % Fe(II) reduced d^{-1}, calculated from the first order rate law: $[Fe(II)_{Tot}](t) = [Fe(II)_{Tot}]_{max}(1-e^{-kt})$, where regression of the measured data produced k = 0.0458 (R^2 = 0.914) and 0.0228 (R^2 = 0.930) for the hematite and goethite experiments, respectively. Instantaneous reduction rates were determined from the first derivative of the first order rate law: $d[Fe(II)_{Tot}]/dt = k[Fe(II)_{Tot}]_{max}(e^{-kt})$.

[b]Fe_{reac} is the total reactive Fe pool, based on the components that were open to isotopic exchange: $Fe(II)_{aq} + Fe(II)_{sorb} + Fe(III)_{reac}$. Fe_{Tot} is the total Fe in the experimental system.

[c]FO is the ferric oxide/hydroxide, either hematite or goethite.

[d]2σ errors were generated by the *Excel* add-in *Isoplot (58)*, based on uncertainties in isotopic measurements and the fraction of Fe(II) in the HCl extractions.